Crystal Structure of Anion-Radical Salts of 7,7,8,8-Tetracyanoquinodimethane with N-xylyl-pyridinium and N-xylyl-isoquinolinium Cations

T. N. Starodub[a,*], D. Fenske[b,c,d], O. Fuhr[b,c], V. O. Yaroshenko[e,f], and D. Stepen'[a]

[a] *Institute of Chemistry, Jan Kochanowski University, Kielce, 25-406 Poland*

[b] *Institute of Inorganic Chemistry, Karlsruhe Institute of Technology, Karlsruhe, 76131 Germany*

[c] *Institute of Nanotechnology (INT) and Karlsruhe Nano Micro Facility (KNMF), Karlsruhe Institute of Technology (KIT), Eggenstein-Leopoldshafen 76344, Germany*

[d] *Lehn-Institute for Functional Materials, School of Chemistry and Chemical Engineering, Sun Yat-Sen University, Guangzhou, 510275 China*

[e] *University of Helsinki, Helsinki, 00014 Finland*

[f] *Matej Bel University, Banská Bystrica, 974 01 Slovakia*

**e-mail: tstarodub@ujk.edu.pl*

Abstract—Novel anion-radical salts of 7,7,8,8-tetracyanoquinodimethane (TCNQ) with N-xylyl-pyridinium and N-xylyl-isoquinolinium cations of complex composition ((N-Xy-Py)$(TCNQ)_2(CH_3CN)$ (**1**) and (N-Xy-iQn)$(TCNQ)_2$ (**2**), respectively) have been synthesized. The crystal and molecular structures of **1** and **2** are determined using X-ray diffraction (XRD) analysis. Salts are crystallized into different systems: the (N-Xy-Py)$(TCNQ)_2(CH_3CN)$ structure belongs to the orthorhombic system, while the (N-Xy-iQn)$(TCNQ)_2$ structure belongs to the triclinic system. Crystals of salt **1** contain dimerized stacks of anion-radicals of the ABAB type, while the stacks in structure **2** are tetramerized. This structural distortion does not facilitate high electrical conductivity, which is confirmed by the IR spectral data: the spectra of salts **1** and **2** do not exhibit any specific features of high-conductivity TCNQ salts (continuous absorption and anomalous line broadening). This fact can be caused by the Peierls instability, which induces dimerization of stacks in crystals of salt **1** and tetramerization of stacks in crystals of salt **2**.

INTRODUCTION

Anion-radical salts (ARSs) based on 7,7,8,8-tetracyanoquinodimethane (TCNQ) are of great interest due to their unusual physical properties [1, 2]. These ARSs are used as conducting materials, which can melt without expansion [1, 3]; magneto-ordered structures (including spin ladders) [1, 4]; and materials for field transistors [1, 5], photodiodes, and other micro- and nanoelectronic devices [1, 2]. The structure and nature of cation affect significantly the physical properties of TCNQ ARSs; therefore, the study of this influence is an urgent task.

In this paper, we report the results of studying the structural and optical properties of TCNQ ARSs with cations based on pyridine and isoquinoline, which become strongly nonplanar after introduction of the corresponding radicals. Novel TCNQ ARSs were synthesized using N-xylyl-pyridinium and N-xylyl-isoquinolinium cations:

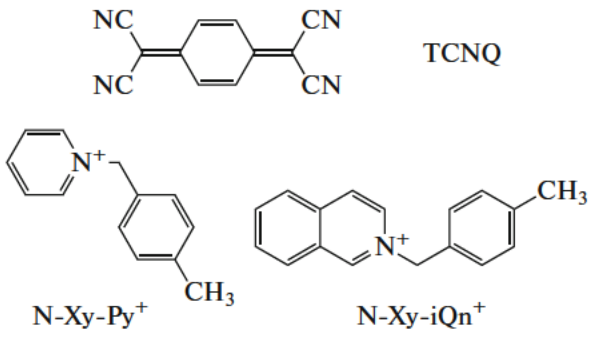

The cations based on pyridine and isoquinoline were chosen due to the fact that, apart from their use as materials of modern electronics and spintronics [2], they are of great biological importance. Organic complexes with pyridine-based cations exhibit antioxidant, antifungal, and antibacterial properties [6]. Isoquinoline-based cations can be used in medicine (e.g.,

for quantitative determination of antibiotics, which decelerate development of gram-positive and gram-negative bacteria, causing skin diseases [7]) and in bio- and nanotechnologies (e.g., for quantitative determination of aliphatic and aromatic amines in water, which is important, because amines are extremely toxic compounds [8, 9]).

EXPERIMENTAL

TCNQ (Aldrich), additionally purified by recrystallization, was used. $(N\text{-}Xy\text{-}Py)^+Br^-$ and $(N\text{-}Xy\text{-}iQn)^+Br^-$ salts were synthesized according to the following reaction:

$$Am + BrCH_2{-}C_6H_4{-}CH_3 \rightarrow (Am{-}CH_2{-}C_6H_4{-}CH_3)^+Br^-,$$
$$Am = Py, isoQn.$$

Alkyl-bromide (0.2 mol) was added in drops to solution of the corresponding amine (0.1 mol) in acetone (200 mL). The mixture was stirred in argon for two to three days (the completeness of quaternization was controlled using paper chromatography). After the completion of reaction, the formed precipitate was filtered, washed with acetone, and dried in vacuum at room temperature (heating leads to decomposition). The obtained salts were not additionally purified.

ARSs **1** and **2** were synthesized according to the following reaction:

$$LiTCNQ + TCNQ + (Am{-}CH_2{-}C_6H_4{-}CH_3)^+Br^- \rightarrow (Am{-}CH_2{-}C_6H_4{-}CH_3)^+(TCNQ)_2^{\bullet -}\downarrow + LiBr.$$

The ARS compositions were determined spectrophotometrically [10] on a Merck Spectroquant Pharo 300 spectrometer. ARSs solutions in acetonitrile in 1-cm-thick cells were used. The obtained results were also confirmed by elemental analysis for carbon, hydrogen, and nitrogen using a VarioMICRO Superuse instrument. According to the data obtained, the ARSs have the following compositions: $(N\text{-}Xy\text{-}Py)(TCNQ)_2(CH_3CN)$ (**1**) and $(N\text{-}Xy\text{-}iQn)(TCNQ)_2$ (**2**).

The calculated values for **1** are as follows: C 73.78, H 4.03, and N 22.17 wt %. The calculated values for $C_{39}H_{25}N_{10}$ are C 73.92, H 3.98, and N 22.10 wt %. The calculated values for **2** are C 76.53, H 3.85, and N 19.68 wt %. The calculated values for $C_{41}H_{24}N_9$ are C 76.62, H 3.76, and N 19.61 wt %.

X-ray diffraction analysis of ARSs **1** and **2** was performed on a Stoe StadiVari Eulerian single-crystal diffractometer at 180 K using a Dectris Pilatus 300K detector with monochromatic MoK_α radiation (λ = 0.71073 Å) and a Dectris EIGER4M detector with GaK_α radiation (λ = 1.34143 Å) for ARSs **1** and **2**, respectively. The crystal structure was resolved according to the method of internal phasing using the ShelXT package [11] and refined according to the full-matrix least-squares method using the SHELXL [12] and OLEX2 [13] programs. All atoms, except for hydrogen, were refined in the anisotropic approximation of displacement parameters. The hydrogen atoms for ARS **2** were localized from the Fourier map and refined independent of other atoms using isotropic displacement parameters, and the hydrogen atoms for ARS **1** were refined using the "rider" model (U_{iso} = $1.5U_{eq}$ for methyl groups and $U_{iso} = 1.2U_{eq}$ for the other groups).

The main crystallographic characteristics and details of the X-ray experiment are listed in Table 1. The structural data were visualized using the Diamond 3.2k program [14]. The molecular structures of the compounds under study are shown in Fig. 1. The experimentally determined bond lengths and angles are given in the ESI (Tables S1–S4).

The crystallographic data were deposited with the Cambridge Crystallographic Data Centre (CCDC nos. 2016745 (ARS **1**) and 1983621 (ARS **2**)) and can be obtained on request at www.ccdc.cam.ac.uk/structures.

The IR absorption spectra of powder samples **1** and **2** were recorded on a Nicoletis 10 instrument (Thermo Scientific) with a Smart MIRacle attachment in the frequency range from 500 to 4000 cm^{-1} at room temperature.

RESULTS AND DISCUSSION

The asymmetric part of unit cells of both ARSs contains an organic cation and two independent radical TCNQ anions (*A* and *B*) (Fig. 1). In addition, the structure of ARS **1** contains an acetonitrile molecule. Based on the formulas of ARSs **1** and **2**, the average charge on $TCNQ^{q-}$ particles should be –0.5 (–1 for two TCNQ particles). However, it is known that the oxidation state of TCNQ affects strongly the bond lengths in it. Taking into account the presence of two crystallographically nonequivalent anion-radicals in the structure, the Kistenmacher relationship

$$q = -41.67[c/(b + d)] + 19.83$$

was used to determine the charge distribution in the TCNQ stacks [15, 16] (Table 2). Different charges of particles of types *A* and *B* were found using the data in Tables S1 and S3. Note that charge disproportionation should increase the resistance in comparison with stacks with identical charges –0.5 on TCNQ particles.

The structures of both ARSs are formed by stacks of TCNQ anion-radicals, between which cations and solvent molecules are located (Fig. 2). This type of packing is characteristic of TCNQ ARSs because of

Table 1. Crystallographic characteristics, details of the X-ray experiment, and structure refinement parameters for ARS (N-Xy-Py)$(TCNQ)_2(CH_3CN)$ (**1**) and (N-Xy-iQn)$(TCNQ)_2$ (**2**)

Compound	**1**	**2**
Empirical formula	$C_{39}H_{25}N_{10}$	$C_{41}H_{24}N_9$
Crystal system, sp. gr., Z	Orthorhombic, $P2_12_12_1$, 4	Triclinic, $P\bar{1}$, 2
T, K	180(1)	180(1)
a, b, c, Å	7.8195(2), 12.6842(5), 32.2214(12)	7.6614(2), 14.5310(4), 15.9062(4)
α, β, γ, deg	90, 90, 90	112.300(2), 91.603(2), 91.492(2)
V, Å^3	3195.85(19)	1636.43(8)
D_{calc}, g/cm^3	1.317	1.304
λ, mm^{-1}	0.083	0.413
Radiation; λ, Å	MoK_α; 0.71073	GaK_α; 1.34143
Diffractometer	Stoe StadiVari Eulerian	
Crystal size, mm	0.38 × 0.1 × 0.03	0.36 × 0.34 × 0.05
T_{min}, T_{max}	0.326, 0.995	0.078, 0.924
Number of reflections: measured/unique, R_{int}/with $I > 2\sigma(I)$	16428/7860, 0.019/6325	22109/7749, 0.016/6479
Number of refined parameters	444	547
$R(F^2)/wR(F^2)$	0.040/0.104	0.035/0.110
S	1.030	1.100
$\Delta\rho_{min}/\Delta\rho_{max}$, e·Å^{-3}	−0.154/0.230	−0.203/0.221
Programs	SHELXL [12], OLEX2 [13]	

the strong interaction of the π-systems of anion-radicals, which usually facilitates high electrical conductivity due to the delocalization of π-electrons.

Stacks of anion-radicals in ARS crystals **1** and **2** are shown in Figs. 3 and 4, respectively. Due to the Peierls and spin-Peierls instability, n-merixation of stacks should occur (here, $1/n$ is the degree of band occupation; in this case, $n = 4$) [1, 2]. In ARS crystals **1**, stacks of anion-radicals are slightly dimerized according to the *ABAB* type, with interplanar distances between neighboring TCNQ particles of 3.24 and 3.32 Å. In ARS crystals **2**, anion-radicals are packed according to the *ABBA* type and tend to be tetramerized (the corresponding $A\cdots B$, $A\cdots A$, and $B\cdots B$ distances are 3.19, 3.32, and 3.36 Å, respectively).

There are very weak hydrogen C–H···N bonds in both crystal structures (the N···H distances lie in the range of 2.47–2.70 Å). One might suggest that it is likely due to packing effects, and the structural elements in the crystal are primarily bound due to the electrostatic interactions between cations and anions and the aforementioned interactions in TCNQ stacks. One should also note the presence of interesting interactions C–H···π: C6–H6*A*...C7–12^i (*i*: 0.5 + x, 1.5 − y, 1 − z) and C5–H5...C11–16^{ii} (*ii*: 2 − x, 1 − y, −z) in structures **1** and **2**, respectively (Fig. 5).

The IR absorption spectra of ARSs **1** and **2** do not contain any specific features, characteristic of high-conductivity TCNQ ARSs (Figs. 6, 7). There are no continuous absorption, corresponding to excitation of conduction electrons, and no lines of intramolecular vibrations, anomalously broadened due to the electron–phonon interaction [1, 2]. A possible reason is the Peierls instability, which induces dimerization of stacks in ARS crystals **1** and tetramerization of stacks in ARS crystals **2**. The IR spectrum of ARS **1** contains a wide band in the range of 3000–3600 cm^{-1}, peaking at 3409 cm^{-1} (Fig. 6). According to [17], this band can

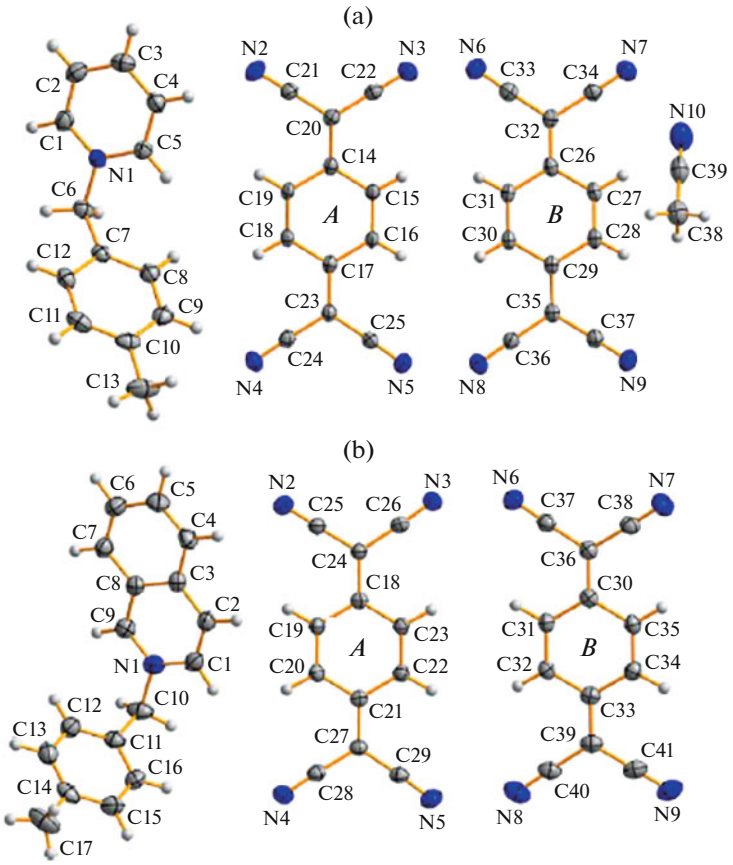

Fig. 1. Molecular structures and enumeration scheme in (a) (N-Xy-Py)$(TCNQ)_2(CH_3CN)$ and (b) (N-Xy-iQn)$(TCNQ)_2$ ARSs.

be related to the charge-transfer band in TCNQ stacks. As follows from Table 2, this corresponds to the transition

$$\ldots(TCNQ^{-0.66})(TCNQ^{-0.29})\ldots$$
$$\rightarrow \ldots(TCNQ^{-0.29})(TCNQ^{-0.66})\ldots$$

Table 2. Analysis of bond lengths in TCNQ and correlation between the bond lengths and charge of TCNQ particles

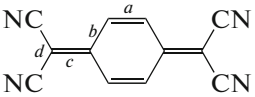

	a	*b*	*c*	*d*	*b* − *c*	*c* − *d*	*c*/(*b* + *d*)	*Q*
$TCNQ^0$	1.345	1.448	1.374	1.441	0.074	−0.067	0.476	−0.001
$TCNQ^{-0.5}$	1.354	1.434	1.396	1.428	0.040	−0.032	0.488	−0.500
$TCNQ^-$	1.374	1.423	1.420	1.416	0.003	0.004	0.500	−0.999
			(**1**)					
TCNQ *A*	1.356	1.431	1.404	1.425	0.027	−0.021	0.492	−0.660
TCNQ *B*	1.351	1.441	1.387	1.431	0.054	−0.044	0.483	−0.290
			(**2**)					
TCNQ *A*	1.365	1.426	1.412	1.421	0.014	−0.009	0.496	−0.830
TCNQ *B*	1.354	1.442	1.388	1.431	0.054	−0.044	0.483	−0.300

All distances are averaged and calculated using the experimental data for the corresponding bonds, with errors disregarded.

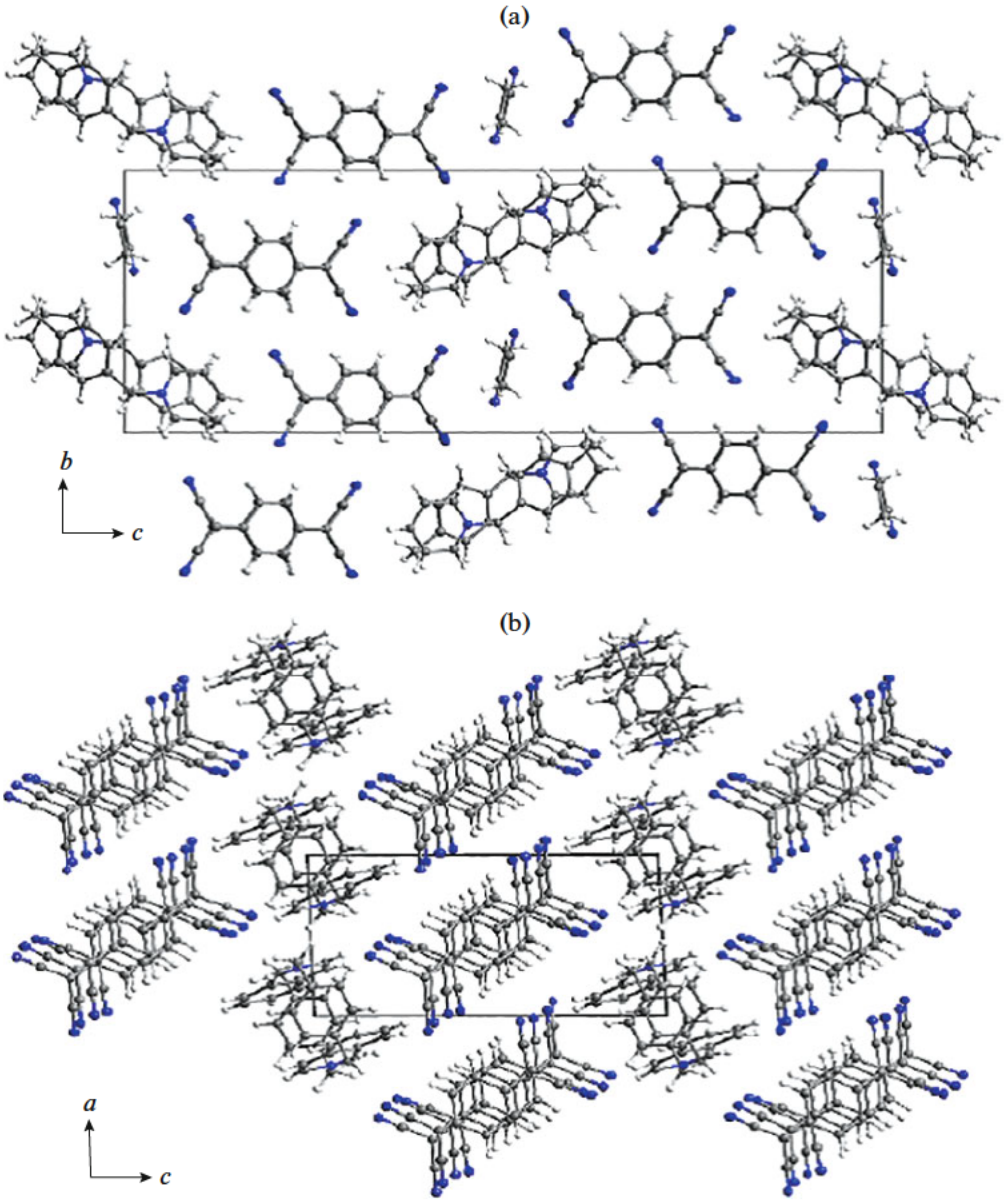

Fig. 2. Crystal structures of (a) (N-Xy-Py)$(TCNQ)_2(CH_3CN)$ and (b) (N-Xy-iQn)$(TCNQ)_2$ ARSs.

Based on the IR spectra, one can estimate the band gap related to the Peierls transition as 0.42 eV. This value corresponds to the energy gain as a result of the transition from homogeneous TCNQ stacks to dimerized stacks.

CONCLUSIONS

Two new TCNQ ARSs with cations containing para-xylyl radicals were synthesized. Both salts belong to salts of complex composition: (N-Xy-Py)$(TCNQ)_2(CH_3CN)$ and (N-Xy-iQn)$(TCNQ)_2$. Despite the weak difference in the cation compositions, the structures of novel ARSs differ. (N-Xy-Py)$(TCNQ)_2(CH_3CN)$ and (N-Xy-iQn)$(TCNQ)_2$ ARSs are crystallized into the orthorhombic and triclinic systems, respectively.

In the structures of ARS **1** and **2**, TCNQ stacks are dimerized and tetramerized, respectively. According to the IR spectroscopy data, both ARSs are low-conducting: continuous absorption, caused by excitation of conduction electrons, and lines anomalously broadened due to the electron–phonon interaction are absent in their spectra.

The IR spectrum of (N-Xy-Py)$(TCNQ)_2(CH_3CN)$ ARS contains a strong wide band in the range of 3000–3600 cm^{-1}, which corresponds to charge-trans-

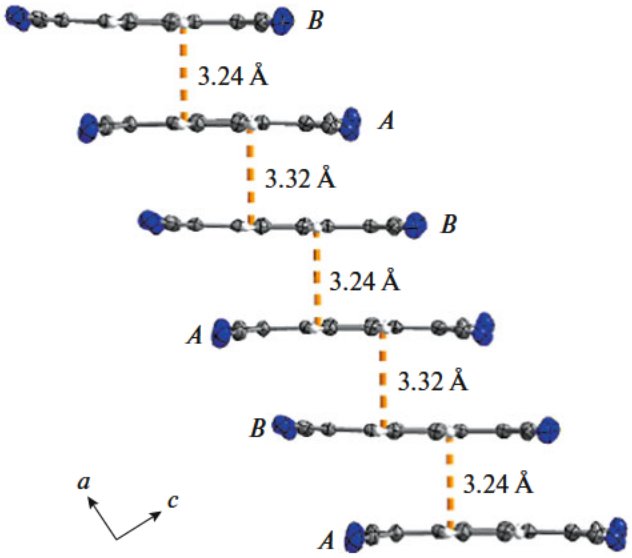

Fig. 3. Stacks of TCNQ anion-radicals along the *a* axis in ARS **1**.

fer excitation in TCNQ stacks. The energy gain due to the Peierls transition is 0.42 eV.

The results obtained enrich the knowledge of the chemistry of TCNQ and related ARSs and may stimulate further studies of salts of 7,7,8,8-tetracyanoquinodimethane with cations based on pyridine and isoquinoline derivatives, which, in turn, may induce discovery of new organic conductors based on TCNQ ARSs.

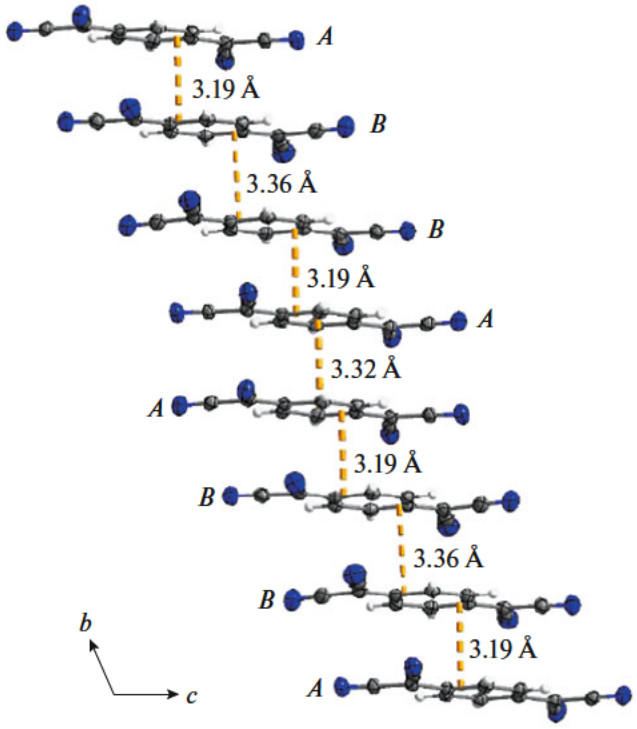

Fig. 4. Stacks of TCNQ anion-radicals along the *b* axis in ARS **2**.

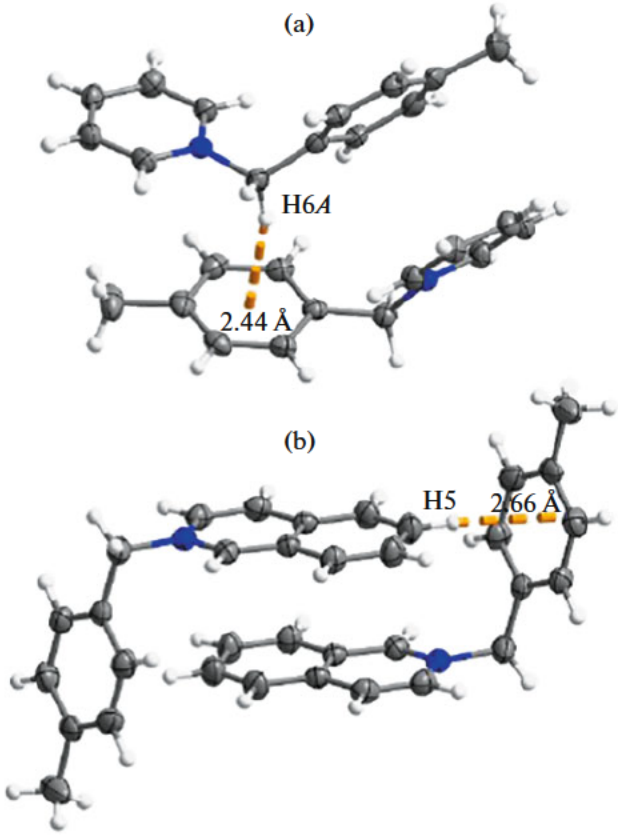

Fig. 5. C–H···π interaction in crystals (a) **1** and (b) **2**.

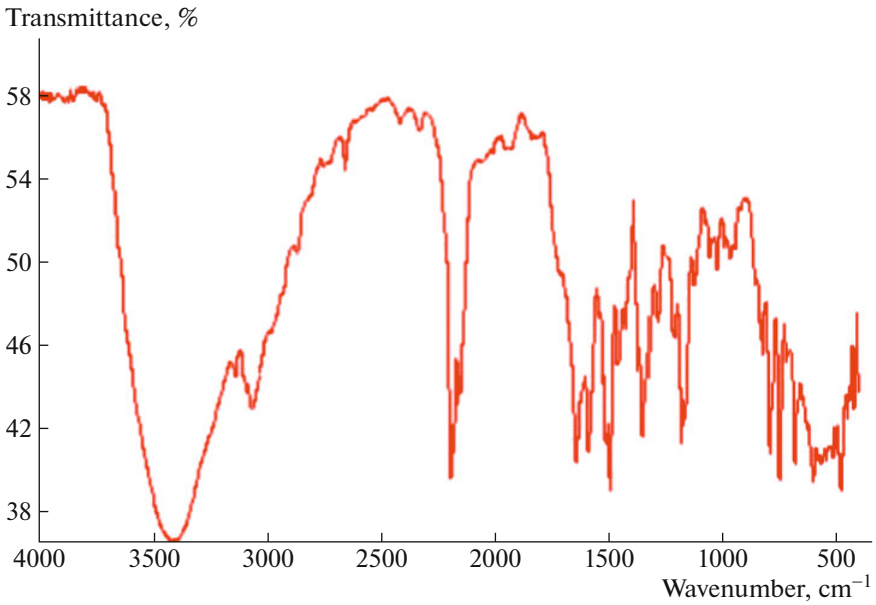

Fig. 6. IR spectrum of ARS **1**.

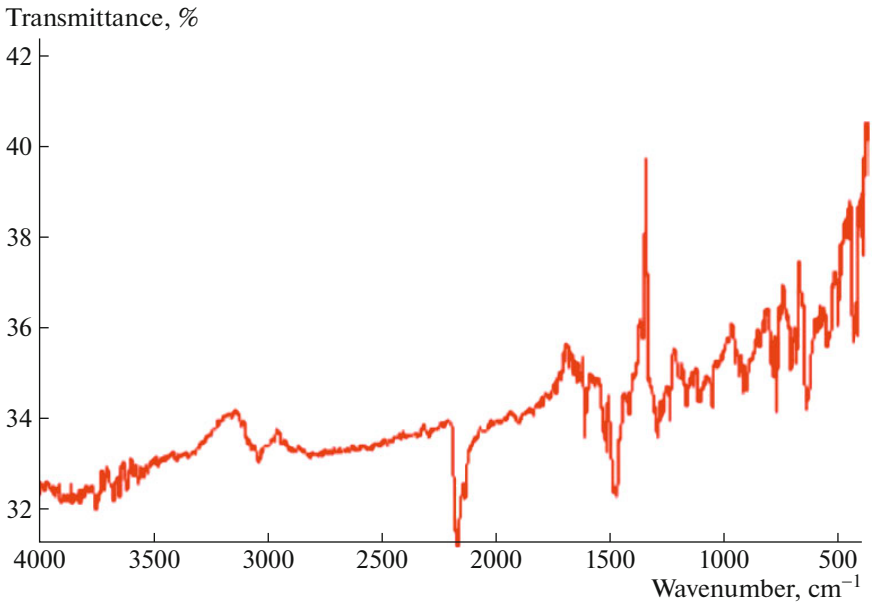

Fig. 7. IR spectrum of ARS **2**.

FUNDING

PhD V.O. Yaroshenko acknowledges the support of the National Science Center within the SONATA 10 program (grant no. 2015/19/D/ST5/02774).

CONFLICT OF INTEREST

The authors declare that they have no conflicts of interest.

REFERENCES

1. V. A. Starodub and T. N. Starodub, Russ. Chem. Rev. **83**, 391 (2014). https://doi.org/10.1070/RC2014v083n05ABEH004299
2. V. A. Starodub, T. N. Starodub, O. N. Kazheva, and V. I. Bregadze, *Materials of Modern Electronics and Spintronics* (Fizmatlit, Moscow, 2018) [in Russian], p. 424.

3. G. Saito and T. Murata, Philos. Trans. R. Soc. **366**, 139 (2008). https://doi.org/10.1098/rsta.2007.2146
4. K. Ueda, T. Sugimoto, S. Endo, et al., Chem. Phys. Lett. **261**, 295 (1966). https://doi.org/10.1016/0009-2614(96)00982-7
5. E. Menard, V. Podzorov, S.-H. Hur, et al., Adv. Mater. **16**, 2097 (2004). https://doi.org/10.1002/adma.200401017
6. A. Piotrowska, J. Drzeżdżon, D. Jacewicz, and L. Chmurzyński, Wiadomości Chemiczne **71**, 220 (2017).
7. W. Martindale, *The Extra Pharmacopoeia,* Vol. 33 (Royal Pharmaceutical Society, London, 2020) [in Russian].
8. T. N. Al-Sabha and N. M. Al-Karemy, J. Anal. Methods Chem. **2013**, 1 (2013).
9. Ch. Wang, Wu, Daniel. L. Jacobs, et al., Chem. Commun. **53**, 1132 (2017).
10. V. A. Starodub, E. M. Gluzman, and Yu. A. Kaftanova, J. Olejniczak. Theor. Experim. Chem. **33**, 95 (1997). https://doi.org/10.1007/BF02765953
11. G. M. Sheldrick, Acta Crystallogr. A **71**, 3 (2015). https://doi.org/10.1107/S2053273314026370
12. G. M. Sheldrick, Acta Crystallogr. C **71**, 3 (2015). https://doi.org/10.1107/S2053229614024218
13. O. V. Dolomanov, L. J. Bourhis, R. J. Gildea, et al., J. Appl. Crystallogr. **42**, 339 (2009). https://doi.org/10.1107/S0021889808042726
14. K. Brandenburg, *Diamond 3.2k* (Crystal Impact GbR, Bonn, Germany (1999).
15. Ö. Üngor, H. Phan, E. Sang Choi, et al., J. Magn. Magn. Mater. **497**, 165984 (2020). https://doi.org/10.1016/j.jmmm.2019.165984
16. Th. J. Kistenmacher, Th. J. Emge, A. N. Bloch, and D. O. Cowan, Acta Crystallogr. B **38**, 1193 (1982). https://doi.org/10.1107/S0567740882005275
17. I. Shirotani and N. Sakai, J. Solid State Chem. **18**, 17 (1976). https://doi.org/10.1016/0022-4596(76)90074-8

Translated by Yu. Sin'kov